

Article

# The Application of a Modified Version of the SWAT Model at the Daily Temporal Scale and the Hydrological Response unit Spatial Scale: A Case Study Covering an Irrigation District in the Hei River Basin

Zheng Wei <sup>1,2,\*</sup>, Baozhong Zhang <sup>1,2,\*</sup>, Yu Liu <sup>1,2</sup> and Di Xu <sup>1,2</sup>

<sup>1</sup> State Key Laboratory of Simulation and Regulation of Water Cycle in River Basin, China Institute of Water Resources and Hydropower Research, Beijing 100038, China; liuyu@iwhr.com (Y.L.); xudi@iwhr.com (D.X.)

<sup>2</sup> National Center of Efficient Irrigation Engineering and Technology Research, Beijing 100048, China

\* Correspondence: weiz1983@126.com (Z.W.); zhangbz@iwhr.com (B.Z.); Tel.: +86-10-6878-5226 (Z.W.)

Received: 1 May 2018; Accepted: 31 July 2018; Published: 10 August 2018



**Abstract:** As a well-built, distributed hydrological model, the Soil and Water Assessment Tool (SWAT) has rarely been evaluated at small spatial and short temporal scales. This study evaluated crop growth (specifically, the leaf area index and shoot dry matter) and daily evapotranspiration at the hydrological response unit (HRU) scale, and SWAT2009 was modified to accurately simulate crop growth processes and major hydrological processes. The parameters of the modified SWAT2009 model were calibrated using data on maize for seed from 5 HRUs and validated using data from 7 HRUs. The results show that daily evapotranspiration, shoot dry matter and leaf area index estimates from the modified SWAT2009 model were satisfactory at the HRU level, and the *RMSE* values associated with daily evapotranspiration, shoot dry matter, and leaf area index were reduced by 17.0%, 1.6%, and 71.2%, compared with SWAT2009. Thus, the influences of various optimal management practices on the hydrology of agricultural watersheds can be effectively assessed using the modified model.

**Keywords:** calibration; irrigation district; evapotranspiration; crop growth; validation

## 1. Introduction

An irrigation district is a composite ecosystem with anthropogenic and natural elements [1]. In an irrigation district, the processes of artificial irrigation and evapotranspiration are critical for water resource management and are important in the hydrological cycle. To understand and analyse watershed processes and interactions, assess management scenarios, test research hypotheses, and evaluate the influence of changing irrigation [2], a coupled hydro-agronomic model is needed.

Numerous agricultural watershed models, such as the Agricultural Non-Point Source (AGNPS) model [3] and Soil and Water Assessment Tool (SWAT) [4,5], have been used to support water quality management, water resource analysis, and soil erosion assessment in agricultural watersheds. Among these models, SWAT is one of the best for the long-term simulation of watersheds dominated by agricultural land use. For example, SWAT has been used to evaluate the influence of irrigation diversion on river flow [4,6–9], to simulate climate change and the associated effects under various scenarios [10,11], to calculate nutrient and sediment yields [12], and to estimate the water balance [13]. SWAT can be effectively calibrated, by comparing the sediment yield and/or simulated surface runoff and nutrient concentrations in runoff to observations at the outlets of watersheds at the subbasin level or at large spatial scales [7,14–18]. The modified SWAT model was developed to improve the

simulation of particular watershed processes. Additionally, the modified version includes enhanced flow predictions (including interflow and percolation, as well as hydraulic conductivity), the evaluation of phosphorus derived from bank erosion in the upper soil layers, organic nitrogen losses, fast percolation, a groundwater dynamics sub-model, amended dynamic functions for crop growth, and channel and drainage losses [12,19–27].

Many studies of runoff hydrological processes have been performed using the SWAT model, but crop growth dynamics (represented by metrics such as shoot dry matter and the leaf area index) and evapotranspiration ( $ET_c$ ) are more significant than rainfall–runoff processes in irrigation districts. Notably, additional studies must be performed in irrigation districts. First,  $ET_c$  simulations have yielded satisfactory results at the field spatial scale and the daily temporal scale. Many studies have described the dual crop coefficients of many crops, such as cotton, winter wheat, maize, sorghum and soybean [28–33]. In SWAT, studies have used satellite-estimated monthly evapotranspiration values to calibrate the  $ET_c$  parameters at the subbasin scale [34–37], daily lysimeter evapotranspiration values to test the  $ET_c$  parameters at the subbasin scale [38]. The weekly or daily temporal scales and hydrological response unit (HRU) spatial scales of such studies are coarse. Existing research has shown that SWAT generally underestimates daily and monthly  $ET_c$ . In addition, automatic irrigation in SWAT can be improved to accommodate limited irrigation scheduling strategies by adding parameters that allow irrigation levels to be set as a percentage of  $ET_c$ . Some studies have mentioned potential flaws in SWAT's automatic irrigation capabilities to simulate real irrigation conditions. At present, the irrigation trigger factor of the soil moisture content method is not reported as the percentage of plant water demand option, but as soil water, which is easily ignored [38–40]. Data availability at the daily scale is often limited in hydrological modelling. Notably, more attention should focus on evapotranspiration in various irrigation domains and the validation and calibration of model parameters in combined distributed hydrological models (e.g., SWAT) and dual crop coefficient models (e.g., SIMDualKc). Second, the irrigation quota is limited to the field capacity, and the excess water above the field capacity is returned to the source and is not taken into account in the calculation of the daily soil water balance. In fact, the irrigation quota is always larger than the field capacity, and such a constraint is not suitable for surface irrigation and flooding irrigation. Additionally, various irrigation schedules should be considered in different irrigation domains, and SWAT should be used for various applications, instead of creating a “unified optimum irrigation schedule”, developing methods for “auto-irrigation”, etc., to accurately describe the cyclic processes involved in regional irrigation. Third, while many studies have assessed the crop water productivity index on the basin scale [41,42] and yield predictions on the HRU scale [43], crop growth dynamics have rarely been evaluated at small scales. Fourth, the leaf area index ( $LAI$ ) curve is determined via linear regression after leaf senescence, but this method is not suitable for irrigated crops,  $LAI$  follow and have logistic relationships with climatic and soil variables [44].

The objectives of this paper are as follows: (1) to modify SWAT and improve its ability to model crop growth parameters (shoot dry matter and  $LAI$ ) and daily evapotranspiration; (2) to conduct a sensitivity analysis of the modified model and identify the parameters that strongly influence estimates of crop growth and  $ET_c$ ; and (3) to calibrate and validate the parameters of  $LAI$ , shoot dry matter, and evapotranspiration in the modified model at small spatial (the HRU level) and temporal (daily) scales.

## 2. Materials and Methods

### 2.1. Study Area

The Yinke experimental site is located in an artificial oasis in the central Hei River Basin of Northwest China (Figure 1). The elevation of the basin ranges from 1456 to 1600 m, and the basin encompasses a total irrigation area of 18.65 km<sup>2</sup> (Figure 1). The irrigation water supply is conveyed by the Yinke Canal [45], which is located adjacent to the Hei River and forms part of the irrigation system that connects the southwest region to the northeast region. In 2012, the main cultivated crop was

maize (84.13%). Other land cover types included forestry (0.18%), pasture (0.82%), water (0.69%), and residential land (14.18%). The climate is cold, and the arid region receives a mean annual precipitation of 125 mm. The reference evapotranspiration in the area is 1972 mm. additionally, the mean annual temperature is 6.7 °C, and the temperature difference between winter and summer is large. The soil texture is mainly homogeneous sandy loam with a gravelly bottom layer.

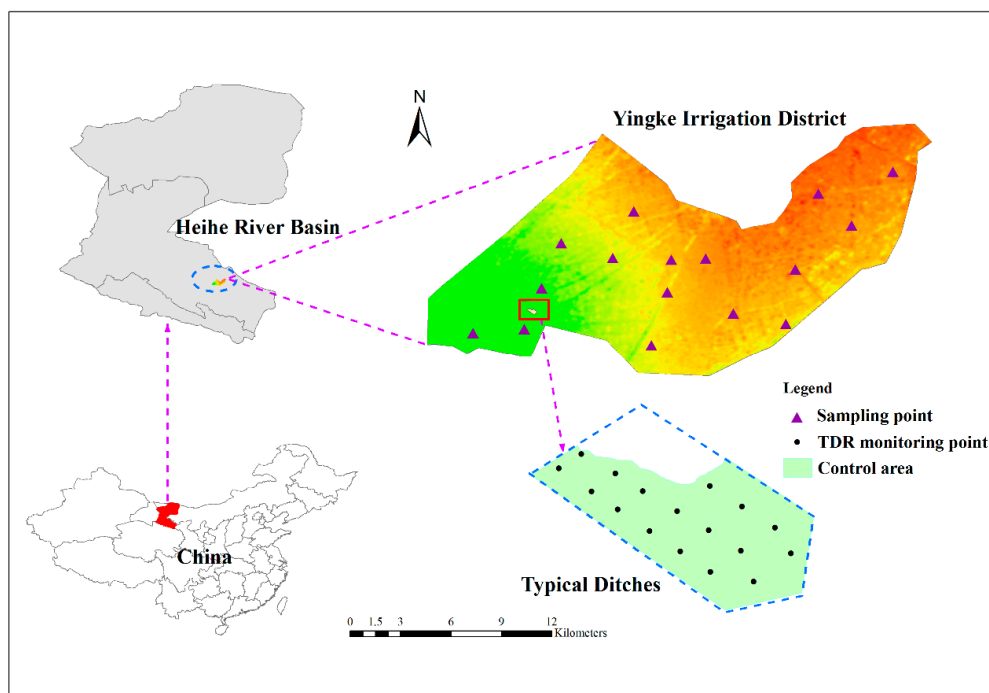


**Figure 1.** Location of the Yinke irrigation district.

## 2.2. Field Experiment

Sixteen points that represent different branch canals and soil types were arranged in the irrigation district, and 17 points that represent typical ditches were arranged in the second rural canal (Figure 1). Maize for seed was the crop chosen for the experiment (local variety name: series 13).

At each monitoring point of the second rural canal, a field soil moisture measurement instrument (TRIME-PICO IPH T3/44) was installed to monitor the soil water profile within each 0.2–0.4 m layer at 15-day intervals. At each monitoring point of different branch, oven drying method was used to monitor the soil water profile at 15-day intervals. The *LAI* and shoot dry matter were included in the crop growth observations. The assessments of *LAI* and biomass were conducted at 15-day intervals. The application ratios of fertilizer were 180 kg/ha for N and 150 kg/ha for P, which were implemented based on local fertilizer management practices [46]. An eddy covariance (EC) instrument was established to measure the latent heat flux at 100°24'37'' E 38°51'25'' N and an elevation of 1519 m. The raw EC data were collected at a sampling frequency of 10 Hz, and they were processed using the post-processing software EdiRe [47].

## 2.3. Model Description

### 2.3.1. SIMDualKc Model

The SIMDualKc model calculates daily crop evapotranspiration by considering soil evaporation and crop transpiration components according to the water balance and the dual coefficient method. The SIMDualKc software application was developed over a range of cultural practices and to provide

$ET_c$  information for use in irrigation scheduling and hydrologic water balances [48]. The actual crop evapotranspiration in the model can be computed as follows:

$$ET_c = (K_s K_{cb} + K_e) ET_0 \quad (1)$$

where  $K_s$  is the water stress coefficient,  $K_e$  is the soil evaporation coefficient, and  $K_{cb}$  is the basal crop coefficient. Additionally,  $ET_0$  is the reference evapotranspiration (mm/d) [49].

The SIMDualKc model, described in the companion paper, was developed to compute crop  $ET_c$  using many recent refinements [50]. The SIMDualKc model calibration procedure involves the adjustment of standard soil parameters (e.g., readily evaporable water  $REW$ , total evaporable water  $TEW$ , and the depth of the surface soil layer  $Z_e$ ) and crop parameters (e.g.,  $K_{cb}$  and the depletion fraction  $p$ ) to minimize the differences between observed and estimated  $ET_c$  values [29].

### 2.3.2. SWAT Model

SWAT is a temporally continuous, physically-based, and spatially semi-distributed model [51]. A watershed can be categorized into multiple sub-watersheds that can be further divided into particular land/soil utilization characteristic units or HRUs. The water balance of each HRU is based on four volumes of storage, including storage in the soil profile (0–2 m), snow, deep aquifers (>20 m), and shallow aquifers (typically 2–20 m). Chemical loadings, flow generation and the sediment yield were calculated in each HRU, and the resulting loads were routed via ponds, channels, and/or reservoirs to the watershed outlet. The soil profile was further divided into multiple layers with different soil water processes, such as evaporation, infiltration, percolation, lateral flow and plant uptake.

A storage routing method is used in the soil percolation module of SWAT to simulate flow in every soil layer in the root zone. Crop evapotranspiration is simulated as a function of root depth,  $LAI$ , and potential evapotranspiration [52].

Crop evapotranspiration ( $ET_c$ ) can be determined using the Penman-Monteith method, and the surface runoff from daily rainfall was estimated using the modified Soil Conservation Service (SCS) curve number [51].

The distributed modelling was carried out through a coupling of modified SWAT2009 and SIMDualKc model (Figure 2). Measured data (Soil water, daily crop evapotranspiration by EC) in the second rural canal were used to calibrate and validate the SIMDualKc model, measured data (Soil water, crop data) in different branch canals and daily crop evapotranspiration calculated by the SIMDualKc model were used for analysis performance of the modified SWAT2009.

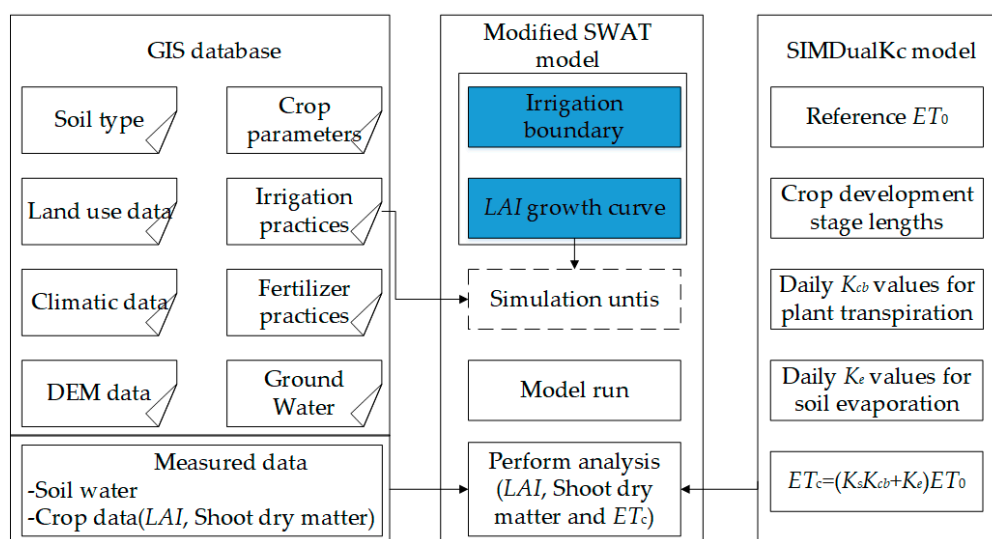


**Figure 2.** Schematic diagram of the coupling modified SWAT2009 and SIMDualKc model.

### 2.3.3. Sensitivity Analysis

The key of SWAT model is the selection of hydrological model parameters. At present, the optimization of SWAT model parameters can be divided into manual adjustment and automatic adjustment. Manual calibration parameters require certain calibration experience of hydrologists, which requires a long working time. Due to the large influence of human interference factors on the model, there is no good evaluation standard. SWAT-CUP can conduct sensitivity analysis, uncertainty analysis and parameter automatic rate determination for the output results of SWAT2009. To assess the parameters that affect crop growth and  $ET_c$  based on daily values, the LH-OAT (Latin Hypercube-One-factor-At-a-Time) method was used in the study, through the LH-OAT, the dominant parameters were determined and a reduction of the number of model parameters was performed [53,54]. The parameters which have influences on crop growth and  $ET_c$  were used for sensitivity analysis are presented in Section 3.3.1.

### 2.4. SWAT Input Data

Three basic files are required to divide the basin into HRUs and subbasins: a digital elevation model (DEM), a soil map and a land use/land cover map. The topographic characteristics (the drainage network, slope length, slope, the number of subbasins and the delimited watersheds) were generated from the DEM of the Hei River Basin (30 × 30 m grid size). The soil and land use data were based on soil distribution maps and crop data obtained from the online portal of the Ecological and Environmental Science Data Centre of Western China. In total, 137 HRUs and 13 subbasins were delineated in the study area (Figure 3). The weather input data, which included minimum and maximum daily air temperatures, relative humidity, wind speed and solar radiation, were obtained from Zhangye meteorological station. This station which is located at 100°25'48'' E 38°55'48'' N and an elevation of 1470 m. Irrigation scheduling was shown in Table 1 for different branch canals, it is reflected in the SWAT input file by setting the \*.mgt files of 13 subbasins separately. The results of the specific settings and process were shown in Figure 3. Current farm management strategies, such as planting and tillage scheduling and harvesting and fertilization practices, were used as inputs to the model.

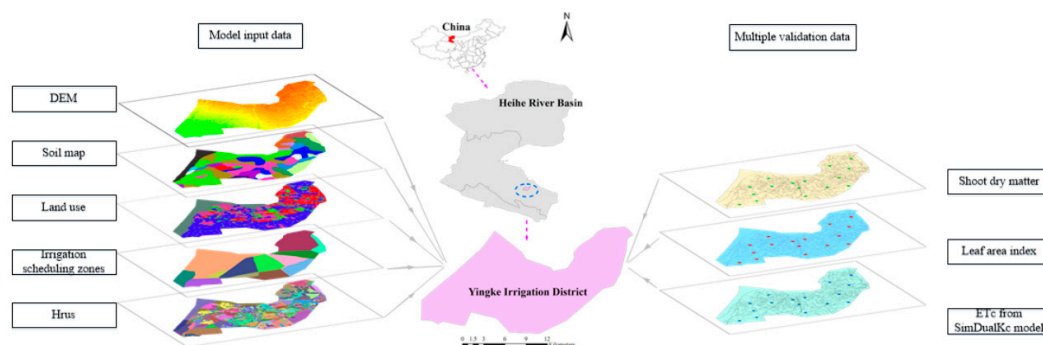


Figure 3. Model input data and multiple validation data.

Table 1. Irrigation quota/irrigation scheduling in the Yingke irrigation district.

Sub Basin	Brach Canals		The Second Rural Canal		
	Irrigation Quota (mm)	Sub Basin	Irrigation Quota (mm)	Irrigation Time (Month/Day)	Irrigation Water (mm)
1	786	8	652	5/26	120
2	786	9	885	6/22	180
3	748	10	861	7/21	160
4	858	11	634	8/13	150
5	1375	12	861		
6	1415	13	1176		
7	652				

## 2.5. Modification of the Model

Since excess irrigation is returned to the source of irrigation instead of being considered in the surface runoff calculations and daily soil water balance calculations, the original version of SWAT2009 could not be used to simulate agricultural irrigation practices [55]. The linear decreasing *LAI* curve after senescence could underestimate  $ET_c$ . Thus, the following modifications were included in the source code of the modified version of SWAT to include the excess water, as previously noted in the soil water balance and *LAI* growth calculations:

1. The maximum amount of water used was in accordance with the depth of irrigation water used in every HRU, as specified by the irrigation operation scheme, rather than the amount of water in the soil profile based on the field capacity by Farida et al. [56]. This modification can be expressed as follows:

Original version:  $vmm = sol\_sumfc$

Modified version:  $vmm = irr\_amt$

where *vmm* refers to the maximum amount of water used (mm); *irr\_amt* refers to the depth of irrigation water used in each HRU (mm), as specified by the user; and *sol\_sumfc* refers to the amount of water in the soil profile at field capacity (mm).

2. *LAI* values had subsequent effects on  $ET_c$  estimation by Gary Marek et al. (2016) [38]. The *LAI* curve after senescence was originally linear, but it should be represented using a logistic growth curve for irrigated crop. This modification can be expressed as follows:

Original version:

$$LAI = \frac{LAI_{mx}}{(1 - fr_{phu, sen})^2} \cdot (1 - fr_{phu})^2, fr_{phu} \geq fr_{phu, sen} \quad (2)$$

Modified version:

$$LAI = \frac{LAI_{mx}}{(1 + a \cdot \exp(1 + b \cdot fr_{phu}))}, fr_{phu} \geq fr_{phu, sen} \quad (3)$$

where *a* and *b* are empirical parameters, *LAI* is the leaf area index on a given day,  $LAI_{mx}$  is the maximum leaf area index,  $fr_{phu}$  is the fraction of potential heat units accumulated by a plant on a given day during the growing season, and  $fr_{phu, sen}$  is the fraction of the growing season (PHU) in which senescence is the dominant growth process.

## 2.6. Model Performance

Three statistical methods and time series plots were used to assess the performance of SWAT and SIMDualKc according to the data. The five statistical criteria used to assess the effectiveness of the validation and calibration results were as follows: (i) the Nash-Sutcliffe efficiency (*NSE*); (ii) the root mean squared error (*RMSE*); and (iii) the coefficient of determination ( $R^2$ ). The calibration objectives for *LAI*, shoot dry matter, and  $ET_c$  were to minimize the *RMSE* and maximize the  $R^2$  and *NSE* values.

## 3. Results

### 3.1. Calibration and Validation of the SIMDualKc Model

#### 3.1.1. Calibration of the SIMDualKc Model

The model simulations were initiated using a table of  $K_{cb}$  values; *p* and soil evaporation parameter values were those recommended by Allen et al. [49]; and the initial  $Z_e$ , *TEW* and *REW* values of 0.1 m, 28 mm and 8 mm, respectively, were used for silt-loam soils. The suggested initial values of  $a_p$  and  $b_p$ ,

which are deep percolation parameters, were 370 and  $-0.0173$ , respectively [57]. The soil parameters were provided in Table 2, and the irrigation schedule was shown in Table 1 for the second rural canal.

The results of comparing the observed and simulated values of available soil water (ASW) based on the calibration data sets of maize for seed are presented in Figure 4. The figure shows that the ASW dynamics were well simulated, and there was no apparent bias in the estimation. The calibrated values of  $K_{cbini}$  and  $p$  exhibited good agreement with those proposed by Allen et al. [49], and the calibrated values of  $K_{cbmid}$  were slightly smaller than those of Allen et al. [49] and Duan et al. [58]. These differences were likely caused by crop and application differences, as this crop was planted for seed and was sent to local companies who buy from the farmers. The reference values discussed above are presented in Table 3.

**Table 2.** Selected soil parameters and values used in SIMDualKc model.

Depth (mm)	Bulk Density (g/cm <sup>3</sup> )	Clay Content (% Soil Mass)	Silt Content (% Soil Mass)	Sand Content (% Soil Mass)
0–200	1.46	13.88	51.17	34.96
200–800	1.48	15.19	50.45	34.36
800–1400	1.57	16.59	50.26	33.16

**Table 3.** Initial and calibrated values of the crop and soil parameters appropriate for maize for seed: crop coefficients, depletion fractions under conditions of no stress, soil evaporation and deep percolation parameters.

	Initial Values	Calibrated Values
Crop coefficients		
$K_{cbini}$	0.15	0.15
$K_{cbdev}$	0.15–1.2	0.15–0.95
$K_{cbmid}$	1.2	0.95
$K_{cbend}$	0.35	0.35
Depletion fractions		
$P_{ini}$	0.5	0.5
$P_{dev}$	0.5	0.5
$P_{mid}$	0.5	0.5
$P_{end}$	0.5	0.5
Soil evaporation		
$REW$ (mm)	8	10
$TEW$ (mm)	28	34
$Z_c$ (m)	0.1	0.15
Deep percolation		
$a_p$	370	366
$b_p$	$-0.0173$	$-0.065$

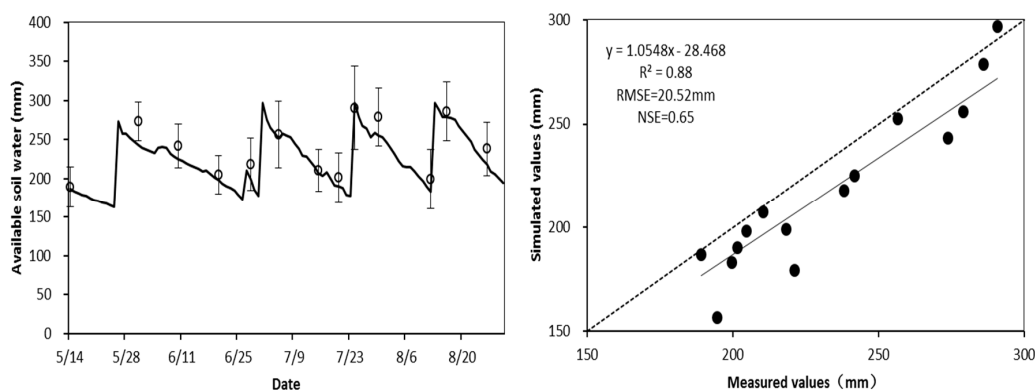


**Figure 4.** Comparison between simulated and observed available soil water of maize for seed.

The results show that the regression coefficient was less than 1.0, indicating that the data plotted slightly below the 1:1 line of the observed data. The coefficient of determination was 0.88, indicating that most of the variance could be explained by the model. The *RMSE* reached 20.52 mm, representing approximately 6.7% of the total available water (*TAW*). Additionally, the *NSE* value was 0.65. The statistical test values of determining coefficient, regression coefficient and intercept are 9.98, 0.52, and 1.14, respectively, with *t*-test ( $t_{0.05} = 2.131, n = 15$ ). The results suggest that the *SIMDualKc* model effectively accounted for the variation in the observed *ASW* and accurately predicted the *ASW* value of maize for seed.

### 3.1.2. Validation of the *SIMDualKc* Model

The results of comparing the observed and simulated  $ET_c$  values are presented in Figure 5. The coefficient of determination was 0.79, indicating that most of the variance could be explained by the model. The *RMSE* reached 1.01 mm/d, and the *NSE* value was 0.56. The statistical test values of determining coefficient, regression coefficient and intercept are 15.55, 11.53, and 8.09, respectively, with *t*-test ( $t_{0.05} = 1.996, n = 67$ ). The results show that there are some schematic errors in the model that can reduce  $ET_c$  predictive power. The observed value  $ET_c$  is the water consumption calculated by the energy balance of the eddy-related system, while the *SIMDualKc* model calculates the  $ET_c$  based on the water balance formula. Results of previous research indicate that the  $ET_c$  calculated by the vorticity correlation system is lower than that calculated by the water balance formula [59], the comparison of  $ET_c$  at different scales may be the main reason of schematic errors.

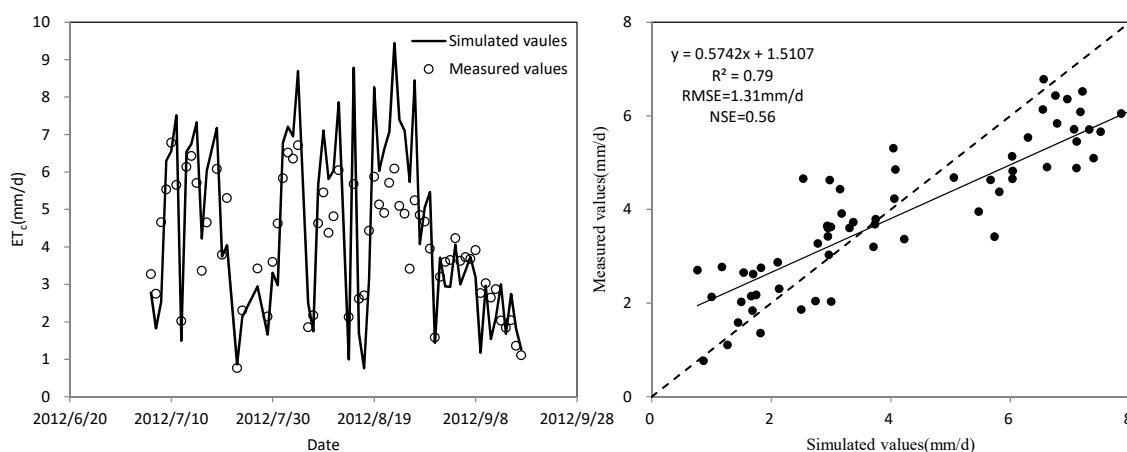


**Figure 5.** Comparison between the simulated and observed  $ET_c$  values of maize for seed.

## 3.2. SWAT2009 vs. Modified SWAT

### 3.2.1. Water Balance

After calibrating and validating SWAT2009 and modified SWAT2009 independently, the irrigation quota of different SWAT versions is shown in Figure 6a, and there were larger differences between SWAT 2009 and modified SWAT2009 versions, the differences ranging from 0–430 mm. The modification of Equation (1) could increase the irrigation water in the soil, and more percolation in the water cycle. In the Figure 6b, there were some differences between modified SWAT2009 and original SWAT2009 versions, and the differences ranged from 46–68 mm. The total evapotranspiration ranged from 540–580 mm of modified SWAT2009, the other is 492–519 mm. Yongyong Zhang et al. (2016) showed that evapotranspiration of seed maize is 545 mm during the growing season [60]. The results is similar with the results of modified SWAT2009 versions. The modification of Equation (2) could increase evapotranspiration, especially after peak *LAI* was reached. In the Figure 6c, there were larger difference between modified SWAT2009 and original SWAT2009 versions, and the differences ranged from –42 to

401 mm. the variation of percolation is similar with the variation of irrigation quota. In the Figure 6d, there were some differences in the senescence stage, the ASW decline rate of modified SWAT2009 was faster than that of original SWAT2009. Therefore, there was a different water balance between modified SWAT2009 and original SWAT2009 versions.

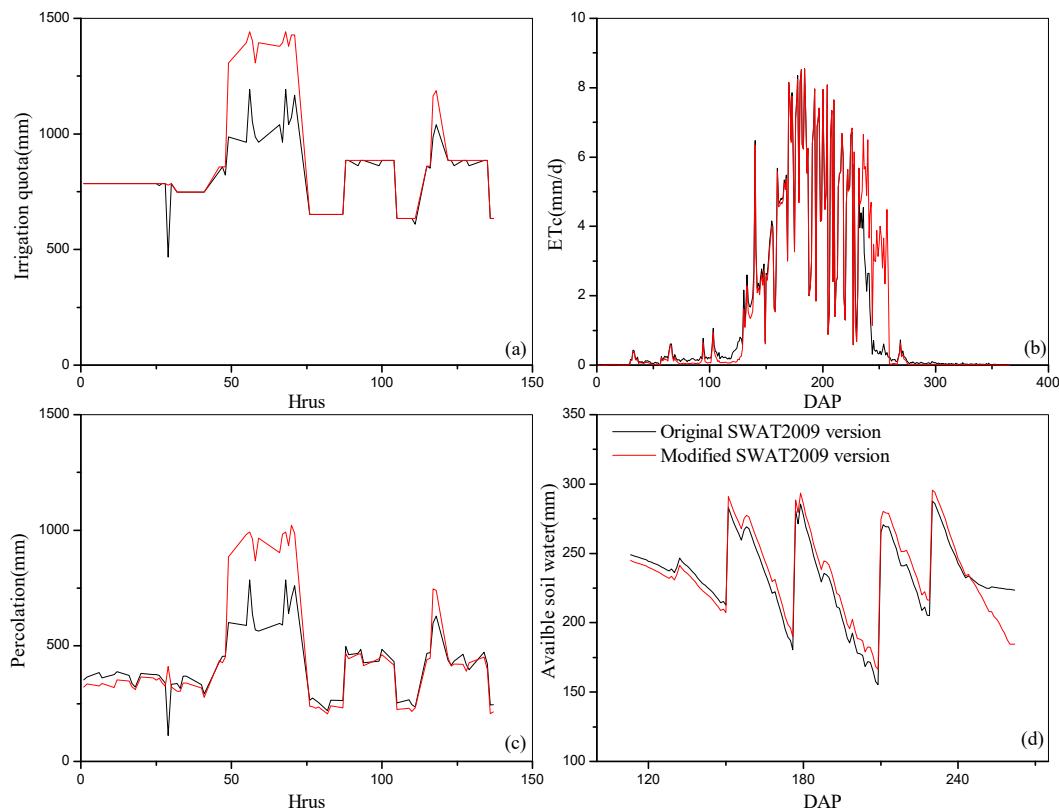


**Figure 6.** Water balance element of different SWAT versions. ((a) irrigation quota; (b) evapotranspiration; (c) percolation; and (d) available soil water).

### 3.2.2. Difference of Model Performance

Crop growth (specifically, the leaf area index and shoot dry matter) and daily evapotranspiration were used to test the SWAT2009 model at the hydrological response unit (HRU) scale, the comparisons between the estimated and measured values of ASW, shoot dry matter, *LAI* and estimated daily  $ET_c$  values using SIMDualKc, SWAT2009, and the modified SWAT model exhibited large differences.

The daily  $ET_c$  results exhibited some differences between the observed data and values simulated using SIMDualKc, SWAT2009, and the modified SWAT model. The less differences were observed for the shoot dry matter and ASW based on SWAT2009 and the modified SWAT2009 model (Table 4). These observations suggest that the parameters values of shoot dry matter and ASW used in the calculation process are nearly equal.

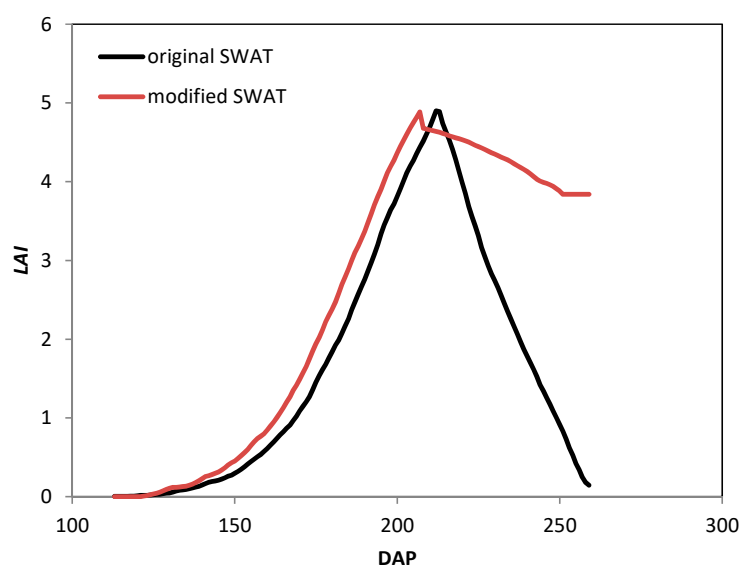
Large differences were observed between SWAT2009 and the modified SWAT model (Figure 7). The largest difference occurred during the leaf senescence stage, when the statistical parameters were much lower than those in the modified SWAT model (Table 4). In SWAT2009, the *RMSE* is 1.84 and the *NSE* is negative. These differences are because of the linear *LAI* functions used in the leaf senescence stage.

Based on this comparison between SWAT2009 and the modified SWAT model, the largest improvement was associated with *LAI*, followed by the  $ET_c$  and available soil water, the values of shoot dry matter were nearly equal in both models.

**Table 4.** Comparison between SWAT2009 and the modified SWAT2009 model.

Parameter	Version	R <sup>2</sup>	RMSE	NSE
Available soil water	SWAT2009	0.71	18.30	0.70
	Modified SWAT2009	0.80	15.98	0.77
Evapotranspiration	SWAT2009	0.35	2.41	0.31
	Modified SWAT2009	0.53	2.00	0.52
Shoot dry matter	SWAT2009	0.89	2.64	0.85
	Modified SWAT2009	0.89	2.60	0.86
LAI	SWAT2009	0.15	1.84	−1.12
	Modified SWAT2009	0.84	0.53	0.82

The units of available water content, evapotranspiration, shoot dry matter, and LAI are mm, mm/d, t/ha, and none, respectively.

**Figure 7.** Variations in the LAI based on the original and modified SWAT models.

### 3.3. Modified SWAT Model Calibration and Validation

#### 3.3.1. Sensitivity Analysis

During the process of simulating LAI using the SWAT model, a sensitivity analysis was performed with the observed data. The results indicated that  $BLAI$ ,  $LAI$ ,  $LAI_{MX2}$ , and  $LAI_{MX1}$  were the primary parameters in the mgt, crop, sol, gw, and rte input files used in the SWAT model (Table 5). Additionally, LAI development depended on the accumulation of plant heat units and the environmental stress indexes. Thus, the shape coefficients are very important for obtaining accurate LAI development curves [55]. In the process of simulating shoot dry matter,  $BIO\_E$ ,  $T\_OPT$ , and  $T\_BASE$  were the primary parameters (Table 6). Biomass production was coupled with the radiation-use efficiency ( $BIO\_E$ ) and intercepted, photosynthetically active radiation [55]. The higher the  $BIO\_E$  value is, the more biomass can be produced [26]. In the process of simulating daily  $ET_c$ ,  $SOL\_K$ ,  $ESCO$  and  $GSI$  were the primary parameters (Table 7).  $ESCO$  is an important parameter used to estimate unsaturated soil evaporation [61], and  $GSI$  is a significant parameter used to calculate  $r_c$  in the Penman-Monteith equation [49]. Additionally,  $ESCO$  is the soil evaporation compensation factor, which affects all the water balance components [62].

**Table 5.** Global sensitivities of the parameters that affect the leaf area index.

Parameter <sup>a</sup>	<i>t</i> -Value <sup>b</sup>	<i>p</i> -Value <sup>c</sup>	Initial Value	Calibrated Value
<i>FRGRW2</i>	1.67	0.09	0.5	0.71
<i>FRGEW1</i>	4.27	<0.01	0.15	0.05
<i>BLAI</i>	9.79	<0.01	6	5.14
<i>DLAI</i>	12.42	<0.01	0.7	0.67
<i>LAI<sub>MX2</sub></i>	18.17	<0.01	0.95	0.77
<i>LAI<sub>MX1</sub></i>	20.11	<0.01	0.05	0.01

<sup>a</sup> Parameter definitions can be found in the theoretical documentation of SWAT [63]. <sup>b</sup> The *t*-value indicates parameter sensitivity; the larger the *t*-value is, the more sensitive the model output is to the parameter. <sup>c</sup> The *p*-value indicates the significance of the *t*-value; the smaller the *p*-value is, the less chance that a parameter has of being falsely identified as sensitive.

**Table 6.** Global sensitivities of the parameters that affect shoot dry matter.

Parameter <sup>a</sup>	<i>t</i> -Value <sup>b</sup>	<i>p</i> -Value <sup>c</sup>	Initial Value	Calibrated Value
<i>HVSTI</i>	0.88	0.38	—	—
<i>USLE_C</i>	1.61	0.11	0.5	0.26
<i>EXT_COEF</i>	1.68	0.09	0.5	0.78
<i>BIO_E</i>	7.15	<0.01	39	28.85
<i>T_OPT</i>	10.58	<0.01	25	23.68
<i>T_BASE</i>	12.36	<0.01	8	12.26

<sup>a</sup> Parameter definitions can be found in the theoretical documentation of SWAT [63]. <sup>b</sup> The *t*-value indicates parameter sensitivity; the larger the *t*-value is, the more sensitive the model output is to the parameter. <sup>c</sup> The *p*-value indicates the significance of the *t*-value; the smaller the *p*-value is, the less chance that a parameter has of being falsely identified as sensitive.

**Table 7.** Global sensitivities of the parameters that affect daily evapotranspiration.

Parameter <sup>a</sup>	<i>t</i> -Value <sup>b</sup>	<i>p</i> -Value <sup>c</sup>	Initial Values	Calibrated Values
<i>ALPHA_BF</i>	0.14	0.89	—	—
<i>GWQMN</i>	0.14	0.89	—	—
<i>SOL_BD</i>	0.22	0.83	—	—
<i>SOL_ZMX</i>	0.31	0.76	—	—
<i>CH_N2</i>	0.33	0.74	—	—
<i>GW_REVAP</i>	0.38	0.70	—	—
<i>CO2HI</i>	0.41	0.68	—	—
<i>CH_K2</i>	0.57	0.57	—	—
<i>GW_DELAY</i>	0.67	0.50	—	—
<i>SOL_AWC_B</i>	0.82	0.41	—	—
<i>CN2</i>	0.82	0.41	—	—
<i>CANMX</i>	0.86	0.39	—	—
<i>SOL_AWC_C</i>	1.39	0.17	0.25	0.20
<i>ALPHA_BNK</i>	1.58	0.11	0.5	0.42
<i>EPCO</i>	1.8	0.07	0.1	0.69
<i>SOL_AWC_D</i>	2.11	0.04	0.18	0.21
<i>SOL_K</i>	5.63	<0.01	20	30
<i>ESCO</i>	3.37	<0.01	0.1	0.57
<i>GSI</i>	23.93	<0.01	0.007	0.01

<sup>a</sup> Parameter definitions can be found in the theoretical documentation of SWAT [63]. <sup>b</sup> The *t*-value indicates parameter sensitivity; the larger the *t*-value is, the more sensitive the model output is to the parameter. <sup>c</sup> The *p*-value indicates the significance of the *t*-value; the smaller the *p*-value is, the less chance that a parameter has of being falsely identified as sensitive.

### 3.3.2. LAI Calibration and Validation

Only those parameters with the highest sensitivities were considered in the calibration process. Table 5 shows the initial values and calibrated values of each parameter considered in the calibration process.

Regional monitoring stations were distributed over 16 HRUs, of which four HRUs were sparsely planted with vegetables (greenhouse crops). Hence, they were not considered in this study. Calibration and validation were performed sequentially [54]. The LAI data from HRU-1, HRU-18, HRU-24, HRU-30, and HRU-58 were adopted for calibration, and the LAI data from HRU-68, HRU-82, HRU-99, HRU-100, HRU-104, HRU-115, and HRU-118 were used for validation.

The calibration and validation curves and statistical parameters are shown in Figure 8 and Table 8, respectively. In the calibration phase, the coefficient of determination ranged from 0.90 to 0.98, the NSE ranged from 0.72 to 0.93, and the RMSE ranged from 0.32 to 0.98. In the validation phase, the coefficient of determination ranged from 0.90 to 0.97, the NSE ranged from 0.22 to 0.89, and the RMSE ranged from 0.41 to 0.95. The simulated and measured LAI values in the calibration and validation phases exhibited good agreement, and the simulated results effectively described the growth process represented by the LAI of maize for seed.

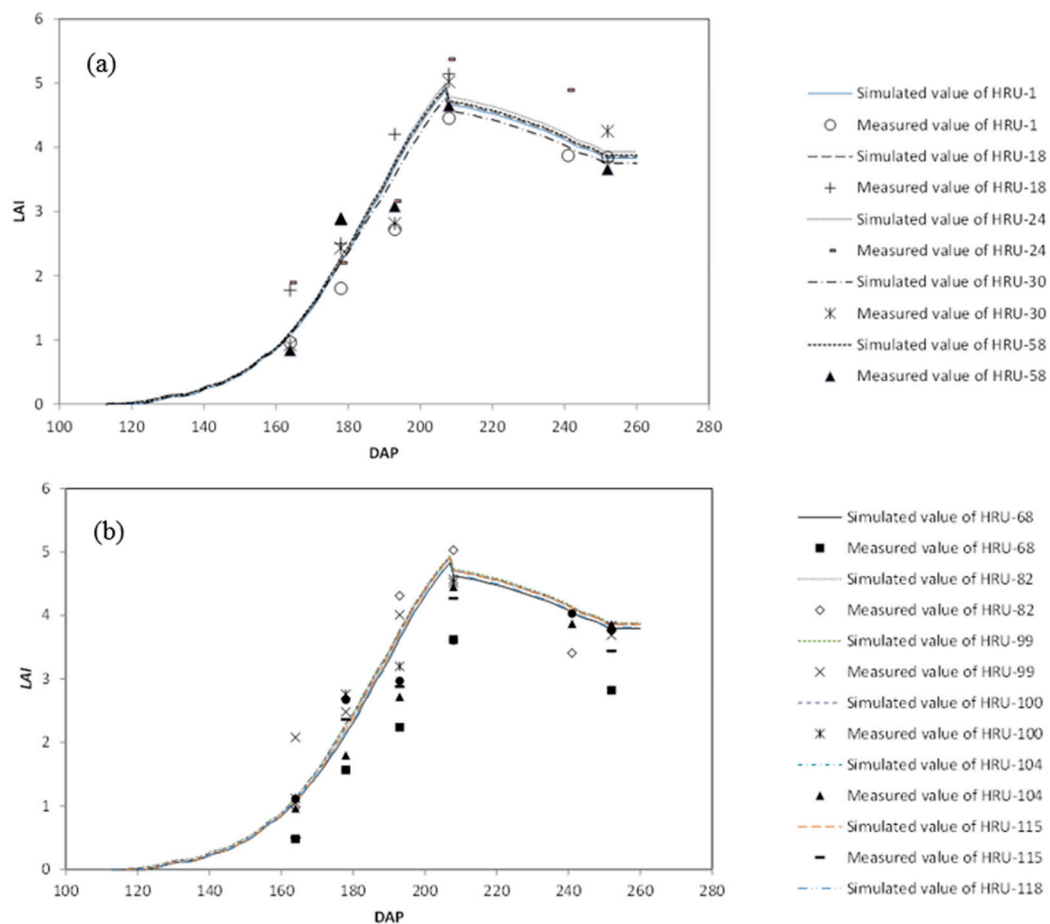


**Figure 8.** Typical variations in simulated and measured LAI values ((a) values for calibration; and (b) values for validation; DAP is day after planting).

**Table 8.** Statistical parameters related to the simulation of *LAI* in the calibration and validation phases.

	HRU	R <sup>2</sup>	RMSE	NSE
Calibration	1	0.94	0.32	0.93
	18	0.96	0.54	0.80
	24	0.85	0.71	0.75
	30	0.81	0.98	0.72
	58	0.89	0.42	0.89
Validation	68	0.96	0.95	0.22
	82	0.88	0.51	0.84
	99	0.81	0.71	0.42
	100	0.84	0.53	0.77
	104	0.94	0.41	0.89
	115	0.94	0.45	0.88
	118	0.85	0.54	0.69

### 3.3.3. Calibration and Validation of Shoot Dry Matter

The default values and adjusted values of each parameter considered in the calibration process are presented in Table 6. The calibrated and validated HRUs were the same as those used in the process of *LAI* calibration and validation. The calibration and validation curves and statistical parameters are shown in Figure 9 and Table 9.

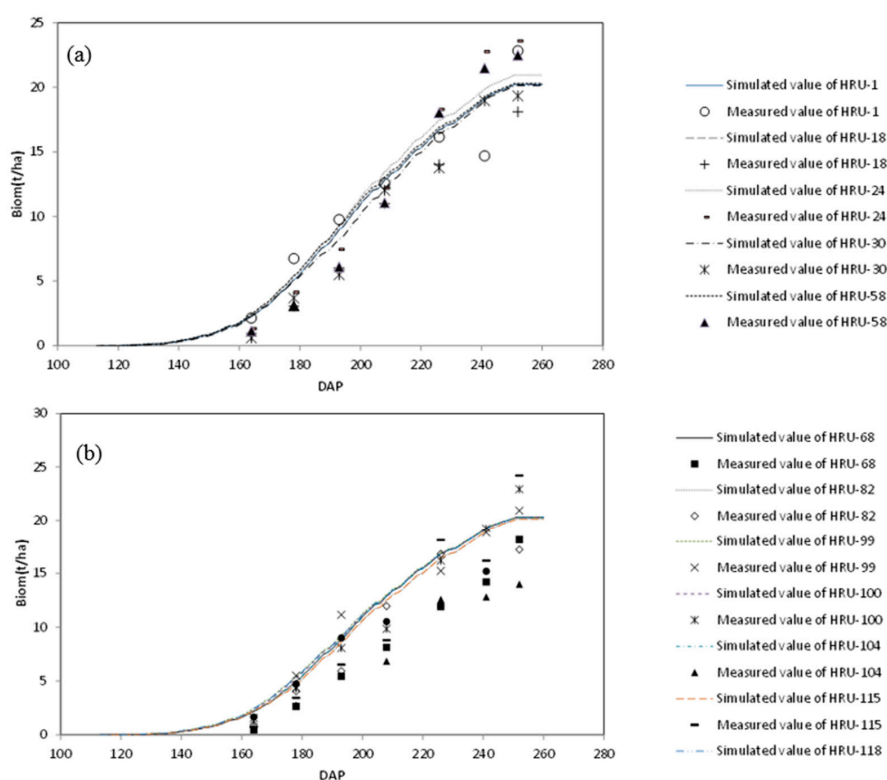


**Figure 9.** Typical variations in simulated and measured values of shoot dry matter ((a) values for calibration; and (b) values for validation; DAP is day after planting).

In the calibration phase, the coefficient of determination between the simulated and measured values of shoot dry matter ranged from 0.92 to 1.0, the *NSE* ranged from 0.66 to 0.97, and the *RMSE* ranged from 1.64 to 5.97 t/ha. In the validation phase, the coefficient of determination ranged from 0.92 to 0.99, the *NSE* ranged from 0.75 to 0.94, and the *RMSE* ranged from 1.14 to 2.91 t/ha. The measured values were consistently less than simulated values for the validation period, the inaccuracy of shoot dry matter estimation might also be caused by the errors in response to soil water stress in the cumulative temperature model.

**Table 9.** Statistical parameters related to shoot dry matter in the calibration and validation phases.

	HRU	R <sup>2</sup>	RMSE (t/ha)	NSE
Calibration	1	0.90	2.89	0.78
	18	0.85	3.58	0.77
	24	0.93	5.07	0.68
	30	0.98	1.64	0.94
	58	0.97	5.97	0.66
Validation	68	0.91	2.55	0.81
	82	0.85	2.91	0.78
	99	0.93	2.17	0.88
	100	0.95	1.14	0.94
	104	0.98	2.65	0.87
	118	0.93	3.19	0.84

### 3.3.4. ET<sub>c</sub> Calibration and Validation

The default values and adjusted values of each parameter considered in the calibration process are presented in Table 7. The HRUs used for calibration and validation were the same as those used in the process of LAI calibration and validation. The calibration and validation curves and statistical parameters are presented in Figures 10 and 11 and Table 10.

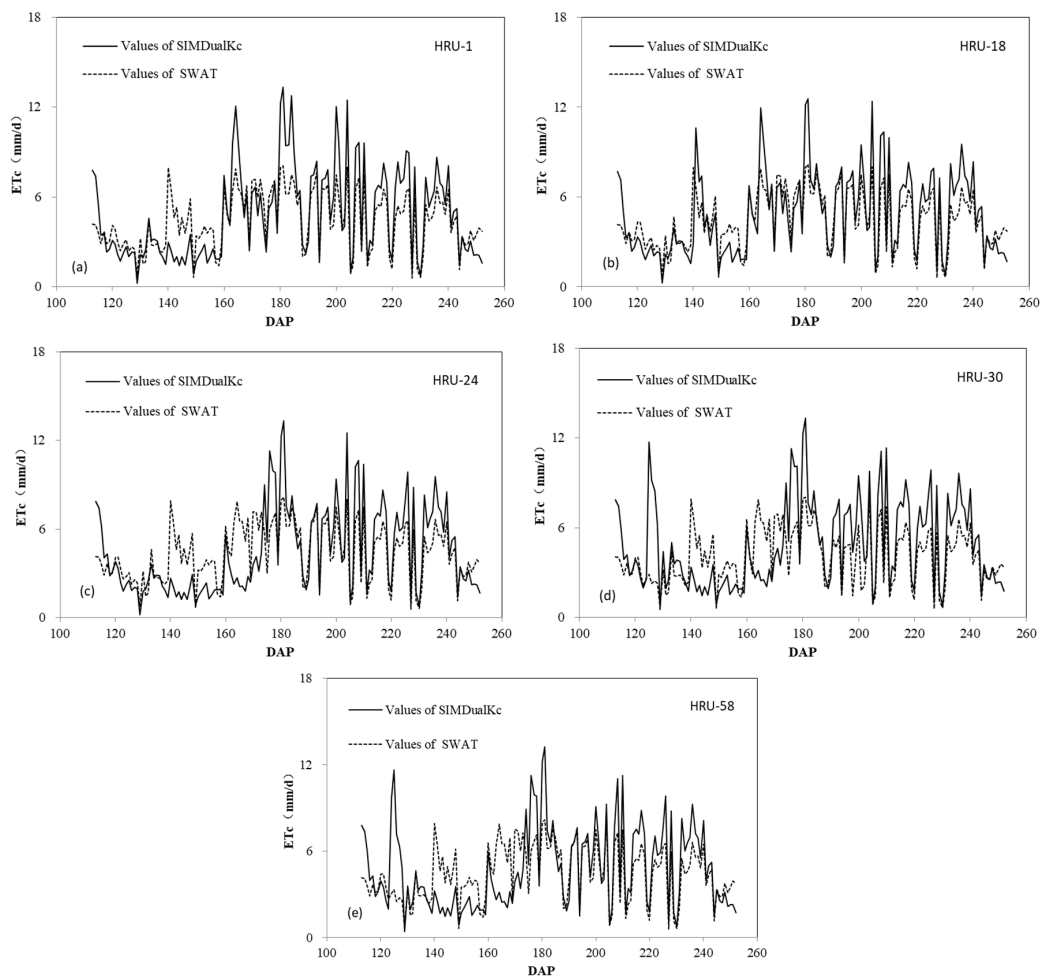


**Figure 10.** Variations in ET<sub>c</sub> simulated using SIMDualKc and SWAT ((a) HRU-1; (b) HRU-18; (c) HRU-24; (d) HRU-30; and (e) HRU-58, which are used for calibration; DAP is day after planting).

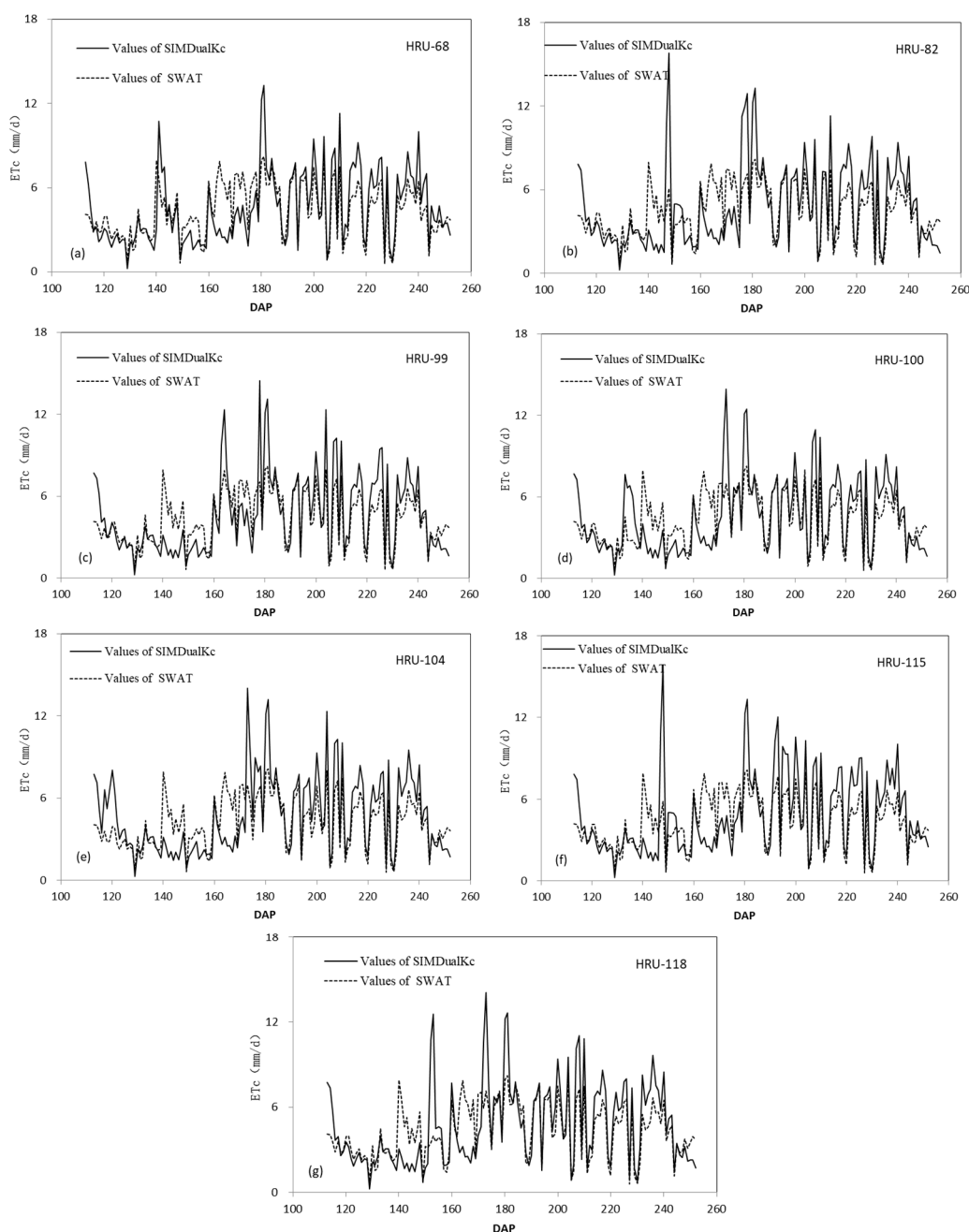


**Figure 11.** Variations in  $ET_c$  simulated using SIMDualKc and SWAT ((a) HRU-68; (b) HRU-82; (c) HRU-99; (d) HRU-100; (e) HRU-104; (f) HRU-115; and (g) HRU-118, which are used for validation; DAP is day after planting).

During the calibration phase, the coefficient of determination between the SIMDualKc and SWAT simulations ranged from 0.62 to 0.86, the *NSE* ranged from 0.33 to 0.70, and the *RMSE* ranged from 1.52 to 2.40 mm/d. Additionally, in the validation phase, the coefficient of determination between the SIMDualKc and SWAT simulations ranged from 0.70 to 0.80, the *NSE* ranged from 0.48 to 0.62, and the *RMSE* ranged from 1.69 to 2.19 mm/d. The  $ET_c$  values simulated by SWAT and SIMDualKc exhibited good agreement in the calibration and validation phases. Marek et al. (2016) showed that The *NSE* value could reach 0.7 in the validation period [38], the inaccuracy of  $ET_c$  estimation might also stem from the errors in the soil water stress function and pre-set GSI.

**Table 10.** Statistical parameters related to  $ET_c$  in the calibration and validation phases.

Phase	HRU	R <sup>2</sup>	RMSE (mm/d)	NSE
Calibration	1	0.71	1.79	0.65
	18	0.74	1.52	0.70
	24	0.51	2.07	0.51
	30	0.39	2.40	0.33
	58	0.42	2.20	0.41
Validation	68	0.59	1.69	0.58
	82	0.52	1.91	0.52
	99	0.49	2.19	0.48
	100	0.64	1.80	0.62
	104	0.52	2.03	0.50
	115	0.51	2.07	0.50
	118	0.49	2.16	0.48

### 3.3.5. Available Soil Water Test

Results showed that the simulated and observed available soil water are in agreement at all observation points (Figure 12). The determination coefficients ranged from 0.56 to 0.96, the regression coefficient ranged from 0.76 to 1.02, RMSE ranged from 7.36 to 25.46 mm, and the average NSE was 0.59, thus indicating that the model explained only a relatively small fraction of observed variance.

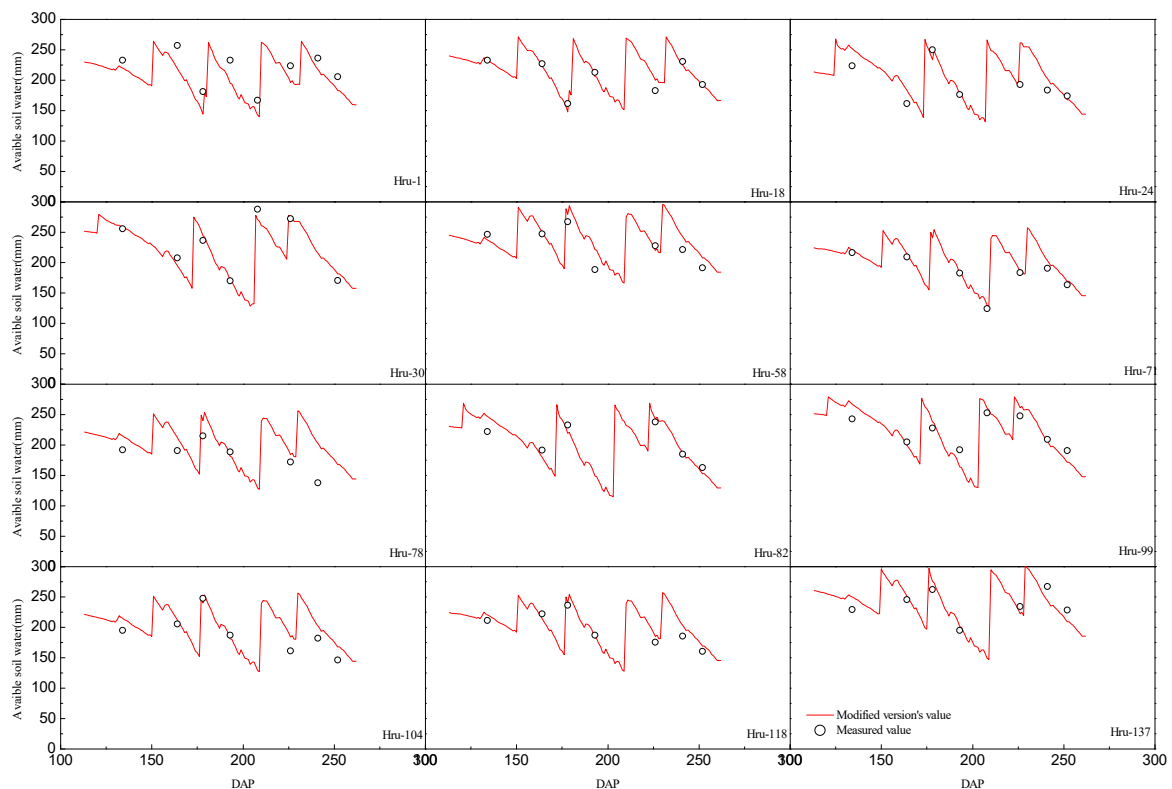


**Figure 12.** Simulated and measured available soil water.

## 4. Discussion

### 4.1. Crop Growth Dynamics

The typical LAI growth patterns (HRU-1) used in the original and modified SWAT models are shown in Figure 7, which illustrates considerable differences in the senescence stage. Since the

original SWAT model uses a linear attenuation formula to simulate the *LAI*, it reflects the dynamics of plant growth under natural conditions but not for agricultural cultivated crops. The parameters were established using empirically fitted functions, although the *LAI* growth-related modules were modified for the senescence phase. Therefore, the growth mechanism of the leaf area was not properly represented. The *LAI* can influence the radiation-use efficiency, which influences the production of biomass because the shape coefficients are flexible in the optimal *LAI* curves [55]. When senescence is the major growth process, other shape coefficients can be used to modify the *LAI* growth sub-module [26]. Notably, the modified sub-module did not consider the effects of nitrogen stresses on leaf senescence. Thus, this process should be added in subsequent studies [14].

The calculation of shoot dry matter in SWAT is based on empirical formulas. Specifically, biomass production is calculated using Beer's law [64], which can assess the proportion of shoots to the total crop biomass. The fraction of roots in the total biomass varies from 0.40 in the emergence stage to 0.20 at maturity. Biomass production can be affected by the light extinction coefficient (*K*), the biomass fraction, and the radiation-use efficiency.

Cabelguenne et al. divided the entire period of crop development into various physiological stages to improve the simulation results and assess differences in water stress between phenological stages [14]. Similarly, future versions of SWAT should consider additional processes related to crop growth to enhance the simulation of crop yields and the yield response to irrigation management.

#### 4.2. Evapotranspiration

According to Figure 11, the  $ET_c$  values simulated using SWAT and SIMDualKc are not identical.  $ET_0$  is the foundation for the calculations of  $ET_c$ . Slight deviations between  $ET_0$  in SWAT and SIMDualKc occur because SWAT uses alfalfa as a reference crop, whereas SIMDualKc  $ET_0$  uses grass. For grass,  $r_s$  equals  $70 \text{ m s}^{-1}$ , and the reference crop height is 0.12 m. For alfalfa,  $r_s$  is  $100 \text{ m s}^{-1}$ , and the reference height is 0.40 m. The input radiation in SWAT was iteratively increased in each subbasin until the value of  $ET_0$  in SWAT matched the value of  $ET_0$  in SIMDualKc to correct these differences. Generally,  $ET_c$  in SIMDualKc is different from  $ET_c$  in SWAT for three potential reasons.

First, one hypothetical conditions are used in SWAT. One condition states that evaporation will decrease firstly if the soil water availability is insufficient (Appendix A, Equation (A1)). The water stress unit (*wstrs*) in SWAT2009 uses the ratio of the actual and maximum plant transpiration (Appendix A, Equation (A2)), an overestimated value of actual plant transpiration will lead to no or little water stress, and the associated material and water cycles are affected.

Second, the *LAI* can affect evapotranspiration when the Penman-Monteith method is used (Appendix A, Equations (A3) and (A4)). In this case, *LAI* decreases linearly in the senescence stage, potentially leading to underestimated values of  $ET_c$ . Gary Marek et al. (2016) also showed that SWAT generally underestimated  $ET_c$  at both the daily and monthly levels [38].

Third, the module that represents agricultural irrigation management in the SWAT model is relatively simple. The effects of irrigation and precipitation on crop transpiration are not effectively reflected in SWAT. Nonetheless, this issue can be resolved in the SIMDualKc model by the daily water balance of the topsoil layer [49]. Although there is inherent uncertainty involved in using this approach, the SWAT model eliminates some of the uncertainty by establishing an upper irrigation limit based on the soil water content.

#### 4.3. Soil Water

In SWAT2009, soil moisture is simulated using the method of layered infiltration, and the model calculates actual crop evapotranspiration based on the available water in different soil layers. The water stress coefficient is then calculated based on the ratio of actual to potential crop evapotranspiration, and this coefficient restricts crop production.

SWAT2009 assumes that water stress occurs when the content of available soil water decreases to  $ASW/4$  (Appendix A, Equation (A5)). Allen et al. and Luo et al. used 0.55 as the threshold value of

soil water stress instead of 0.25 [26,49]. Water extraction decreases below this threshold, despite the differences between crop and soil types. Nonetheless, the soil water holding capacity is varied, based on the different crop and soil types. The water stress coefficient calculated by Equation (A5) uses an exponential formula. There are many applications of the water stress coefficient from FAO56 using the ratio of total and readily available water [49], and from Feddes et al. (1978) considering the effects of water potential on the uptake rate to be multiplicative [65]. The water stress coefficient formula of SWAT should accept more tests for irrigation crops.

## 5. Conclusions

The highest sensitivity parameters are *FRGRW2*, *FRGEW1*, *BLAI*, *DLAI*, *LAI<sub>mx2</sub>*, and *LAI<sub>mx1</sub>* for the leaf area index, *EXT\_COEF*, *BIO\_E*, *T\_OPT*, and *T\_BASE* for the shoot dry matter, *EPCO*, *SOL\_AWC\_D*, *SOL\_K*, *ESCO*, and *GSI* for daily evapotranspiration.

The modified version of the SWAT model exhibits better performance on the daily evapotranspiration, shoot dry matter, and leaf area index at the daily temporal scale and the HRU spatial scale.

Based on the performance statistics of modified SWAT model, there may be errors related to water stress functions in shoot dry matter and  $ET_c$  estimation, and the most important thing is that the stress factor cannot be well reflected into the crop growth. Therefore, users should be aware of the response of crop growth to soil moisture movement.

**Author Contributions:** Z.W. and B.Z. conceived and designed the study. Z.W. wrote the initial draft. Y.L. and D.X. reviewed and revised the manuscript.

**Funding:** This research was supported by the National Key R&D Program of China (2017YFC0403202), the Chinese National Natural Science Fund (91425302, 51479210, and 51379217), IWHR Research & Development Support Program (ID0145B082017 and ID0145B742017), and the Special Fund of State Key Laboratory of Simulation and Regulation of Water Cycle in River Basin, China Institute of Water Resources and Hydropower Research (SKL2018CG).

**Conflicts of Interest:** The authors declare no conflict of interest.

## Appendix A

See Equations (A1)–(A5):

$$\begin{aligned} & \text{if}(pet < es\_max + ep\_max)\text{then} \\ es\_max &= pet \times es\_max / (es\_max + ep\_max) \\ & \text{if}(pet\_day < es\_max + ep\_max)\text{then} \\ es\_max &= pet\_day - ep\_max \end{aligned} \quad (A1)$$

where  $ep\_max$  is the maximum transpiration,  $es\_max$  is the maximum evaporation,  $pet\_day$  is the potential evapotranspiration, and  $pet$  is the amount of  $pet\_day$  remaining after the water stored in the canopy evaporates.

The water stress unit ( $wstrs$ ) in SWAT2009 is as follows:

$$wstrs = 1 - E_{tact} / E_t \quad (A2)$$

where  $E_t$  is the maximum plant transpiration on a given day and  $E_{tact}$  is the actual plant evapotranspiration. The plant transpiration rate and  $wstrs$  range from 0.0 to 1.0 when  $wstrs$  equals 0.0.

$$r_c = \frac{r_1}{0.5 \cdot LAI} \quad (A3)$$

$$\lambda ET_c = \frac{\Delta \cdot R_{net} + \rho \cdot \gamma \cdot \frac{VPD}{r_a}}{\Delta + \gamma \cdot \left(1 + \frac{r_c}{r_a}\right)} \quad (A4)$$

where  $ET_c$  is the daily evapotranspiration ( $\text{mm d}^{-1}$ ),  $\Delta$  is the slope of the saturation vapour pressure-temperature curve ( $\text{kPa } ^\circ\text{C}^{-1}$ ),  $\rho$  is the air density ( $\text{kg m}^{-3}$ ),  $\gamma$  is the psychrometric constant ( $\text{kPa } ^\circ\text{C}^{-1}$ ), VPD is the vapour pressure deficit ( $\text{kPa}$ ),  $r_a$  is the atmospheric resistance ( $\text{s m}^{-1}$ ),  $r_c$  is the canopy resistance ( $\text{s m}^{-1}$ ), and  $r_l$  is the minimum effective stomatal resistance of a single leaf ( $\text{s m}^{-1}$ ).

SWAT2009 assumes that water stress occurs when the available soil water content decreases to  $ASW/4$ :

$$reduc = \exp \left[ 5 \left( \frac{1}{4} \frac{SW_l}{ASW_l} - 1 \right) \right] \text{ when } SW_l \leq \frac{1}{4} ASW_l \quad (\text{A5})$$

where  $SW_l$  refers to the volumetric soil water content above the wilting point,  $reduc$  is the water uptake reduction factor,  $l$  is the number of soil layers, and  $ASW$  is the available soil water.

## References

1. Wang, W.-Y.; Luo, W.; Wang, Z.-R. Surge flow irrigation with sediment-laden water in northwestern China. *Agric. Water Manag.* **2005**, *75*, 1–9. [[CrossRef](#)]
2. He, C. Integration of geographic information systems and simulation model for watershed management. *Environ. Model. Softw.* **2003**, *18*, 809–813. [[CrossRef](#)]
3. Young, R.A.; Onstad, C.; Bosch, D.; Anderson, W. AGNPS: A nonpoint-source pollution model for evaluating agricultural watersheds. *J. Soil Water Conserv.* **1989**, *44*, 168–173.
4. Arnold, J.G.; Allen, P.M.; Bernhardt, G. A comprehensive surface-groundwater flow model. *J. Hydrol.* **1993**, *142*, 47–69. [[CrossRef](#)]
5. Gassman, P.W.; Reyes, M.R.; Green, C.H.; Arnold, J.G. *The Soil and Water Assessment Tool: Historical Development, Applications, and Future Research Directions*; Center for Agricultural and Rural Development, Iowa State University: Heady Hall, IA, USA, 2007.
6. Behera, S.; Panda, R. Evaluation of management alternatives for an agricultural watershed in a sub-humid subtropical region using a physical process based model. *Agric. Ecosyst. Environ.* **2006**, *113*, 62–72. [[CrossRef](#)]
7. Bosch, D.; Sheridan, J.; Batten, H.; Arnold, J. Evaluation of the SWAT model on a coastal plain agricultural watershed. *Trans. ASAE* **2004**, *47*, 1493–1506. [[CrossRef](#)]
8. Santhi, C.; Muttiah, R.; Arnold, J.; Srinivasan, R. A GIS-based regional planning tool for irrigation demand assessment and savings using SWAT. *Trans. ASAE* **2005**, *48*, 137–147. [[CrossRef](#)]
9. Sophocleous, M.; Perkins, S.P. Methodology and application of combined watershed and ground-water models in Kansas. *J. Hydrol.* **2000**, *236*, 185–201. [[CrossRef](#)]
10. Edmonds, J.A.; Rosenberg, N.J. Climate change impacts for the conterminous USA: An integrated assessment summary. In *Climate Change Impacts for the Conterminous USA*; Springer: Berlin/Heidelberg, Germany, 2005; pp. 151–162.
11. Thomson, A.M.; Brown, R.A.; Rosenberg, N.J.; Izaurralde, R.C.; Benson, V. Climate change impacts for the conterminous USA: An integrated assessment. In *Climate Change Impacts for the Conterminous USA*; Springer: Berlin/Heidelberg, Germany, 2005; pp. 43–65.
12. Lenhart, T.; Van Rompaey, A.; Steegen, A.; Fohrer, N.; Frede, H.G.; Govers, G. Considering spatial distribution and deposition of sediment in lumped and semi-distributed models. *Hydrol. Process.* **2005**, *19*, 785–794. [[CrossRef](#)]
13. Cau, P.; Cadeddu, A.; Lecca, G.; Gallo, C.; Marrocu, M. Calcolo del bilancio idrico della regione Sardegna con il modello idrologico SWAT. *L'acqua* **2005**, *5*, 29–38.
14. Cabelguenne, M.; Debaeke, P. Experimental determination and modelling of the soil water extraction capacities of crops of maize, sunflower, soya bean, sorghum and wheat. *Plant Soil.* **1998**, *202*, 175–192. [[CrossRef](#)]
15. Cabelguenne, M.; Jones, C.; Marty, J.; Dyke, P.; Williams, J. Calibration and validation of EPIC for crop rotations in southern France. *Agric. Syst.* **1990**, *33*, 153–171. [[CrossRef](#)]
16. Chanasyk, D.; Mapfumo, E.; Willms, W. Quantification and simulation of surface runoff from fescue grassland watersheds. *Agric. Water Manag.* **2003**, *59*, 137–153. [[CrossRef](#)]
17. Du, B.; Saleh, A.; Jaynes, D.; Arnold, J. Evaluation of SWAT in simulating nitrate nitrogen and atrazine fates in a watershed with tiles and potholes. *Trans. ASAE* **2006**, *49*, 949–959. [[CrossRef](#)]

18. Shrestha, M.K.; Recknagel, F.; Frizenschaf, J.; Meyer, W. Assessing SWAT models based on single and multi-site calibration for the simulation of flow and nutrient loads in the semi-arid Onkaparinga catchment in South Australia. *Agric. Water Manag.* **2016**, *175*, 61–71. [[CrossRef](#)]
19. Van Griensven, A.; Bauwens, W. Multiobjective autocalibration for semidistributed water quality models. *Water Resour. Res.* **2003**, *39*, 1348–1356. [[CrossRef](#)]
20. Van Griensven, A.; Bauwens, W. Application and evaluation of ESWAT on the Dender basin and the Wister Lake basin. *Hydrol. Process.* **2005**, *19*, 827–838. [[CrossRef](#)]
21. Hattermann, F.; Krysanova, V.; Wechsung, F.; Wattenbach, M. Integrating groundwater dynamics in regional hydrological modelling. *Environ. Model. Softw.* **2004**, *19*, 1039–1051. [[CrossRef](#)]
22. Baffaut, C.; Benson, V. Modeling flow and pollutant transport in a karst watershed with SWAT. *Trans. ASABE* **2009**, *52*, 469–479. [[CrossRef](#)]
23. Cau, P.; Paniconi, C. Assessment of alternative land management practices using hydrological simulation and a decision support tool: Arborea agricultural region, Sardinia. *Hydrol. Earth Syst. Sci.* **2007**, *11*, 1811–1823. [[CrossRef](#)]
24. Zheng, J.; Li, G.-Y.; Han, Z.-Z.; Meng, G.-X. Hydrological cycle simulation of an irrigation district based on a SWAT model. *Math. And Comput. Model.* **2010**, *51*, 1312–1318. [[CrossRef](#)]
25. Kannan, N.; Jeong, J.; Srinivasan, R. Hydrologic modeling of a canal-irrigated agricultural watershed with irrigation best management practices: Case study. *J. Hydrol. Eng.* **2010**, *16*, 746–757. [[CrossRef](#)]
26. Luo, Y.; He, C.; Sophocleous, M.; Yin, Z.; Hongrui, R.; Ouyang, Z. Assessment of crop growth and soil water modules in SWAT2000 using extensive field experiment data in an irrigation district of the Yellow River Basin. *J. Hydrol.* **2008**, *352*, 139–156. [[CrossRef](#)]
27. Wang, J.; Cui, Y. Modified SWAT for rice-based irrigation system and its assessment. *Trans. CSAE* **2011**, *27*, 22–28. (In Chinese)
28. Liu, Y.; Pereira, L. Validation of FAO methods for estimating crop coefficients. *Trans. Chin. Soc. Agric. Eng.* **2000**, *16*, 26–30. (In Chinese)
29. Pereira, L.; Cai, L.; Hann, M. Farm water and soil management for improved water use in the North China plain. *Irrig. Drain.* **2003**, *52*, 299–317. [[CrossRef](#)]
30. Liu, Y.; Luo, Y. A consolidated evaluation of the FAO-56 dual crop coefficient approach using the lysimeter data in the North China Plain. *Agric. Water Manag.* **2010**, *97*, 31–40. [[CrossRef](#)]
31. Tolk, J.; Howell, T. Measured and simulated evapotranspiration of grain sorghum grown with full and limited irrigation in three high plains soils. *Trans. ASAE* **2001**, *44*, 1553–1558.
32. Zhao, N.; Liu, Y.; Cai, J.; Paredes, P.; Rosa, R.D.; Pereira, L.S. Dual crop coefficient modelling applied to the winter wheat–summer maize crop sequence in North China Plain: Basal crop coefficients and soil evaporation component. *Agric. Water Manag.* **2013**, *117*, 93–105. [[CrossRef](#)]
33. Odhiambo, L.O.; Irmak, S. Evaluation of the impact of surface residue cover on single and dual crop coefficient for estimating soybean actual evapotranspiration. *Agric. Water Manag.* **2012**, *104*, 221–234. [[CrossRef](#)]
34. Immerzeel, W.; Droogers, P. Calibration of a distributed hydrological model based on satellite evapotranspiration. *J. Hydrol.* **2008**, *349*, 411–424. [[CrossRef](#)]
35. Cai, X.; Xu, Z.; Su, B.; Yu, W. Distributed simulation for regional evapotranspiration and verification by using remote sensing. *Trans. CSAE* **2009**, *25*, 411–424.
36. Qian, K.; Ye, S.; Zhu, Q. Evapotranspiration simulation with different scenarios analyses of Fangshan District by SWAT model. *Trans. CSAE* **2011**, *27*, 99–105.
37. Liu, X.; Wang, S.; Xue, H.; Singh, V.P. Simulating Crop Evapotranspiration Response under Different Planting Scenarios by Modified SWAT Model in an Irrigation District, Northwest China. *PLoS ONE* **2015**, *10*, e0139839. [[CrossRef](#)] [[PubMed](#)]
38. Marek, G.W.; Gowda, P.H.; Evett, S.R.; Baumhardt, R.L.; Brauer, D.K.; Howell, T.A.; Marek, T.H.; Srinivasan, R. Estimating Evapotranspiration for Dryland Cropping Systems in the Semiarid Texas High Plains Using SWAT. *J. Am. Water Resour. Assoc.* **2016**, *52*, 298–314. [[CrossRef](#)]
39. Marek, G.W.; Gowda, P.H.; Marek, T.H.; Porter, D.O.; Baumhardt, R.L.; Brauer, D.K. Modeling long-term water use of irrigated cropping rotations in the Texas High Plains using SWAT. *Irrig. Sci.* **2017**, *35*, 111–123. [[CrossRef](#)]

40. Chen, Y.; Marek, G.W.; Marek, T.H.; Brauer, D.K.; Srinivasan, R. Assessing the Efficacy of the SWAT Auto-Irrigation Function to Simulate Irrigation, Evapotranspiration, and Crop Response to Management Strategies of the Texas High Plains. *Water* **2017**, *9*, 509. [[CrossRef](#)]
41. Ahmadzadeh, H.; Morid, S.; Delavar, M.; Srinivasan, R. Using the SWAT model to assess the impacts of changing irrigation from surface to pressurized systems on water productivity and water saving in the Zarrineh Rud catchment. *Agric. Water Manag.* **2015**, *175*, 15–28. [[CrossRef](#)]
42. Huang, F.; Li, B. Assessing grain crop water productivity of China using a hydro-model-coupled-statistics approach: Part I: Method development and validation. *Agric. Water Manag.* **2010**, *97*, 1077–1092. [[CrossRef](#)]
43. Sinnathamby, S.; Douglas-Mankin, K.R.; Craige, C. Field-scale calibration of crop-yield parameters in the Soil and Water Assessment Tool (SWAT). *Agric. Water Manag.* **2017**, *180*, 61–69. [[CrossRef](#)]
44. Luo, T.; Pan, Y.; Ouyang, H.; Shi, P.; Luo, J.; Yu, Z.; Lu, Q. Leaf area index and net primary productivity along subtropical to alpine gradients in the Tibetan Plateau. *Glob. Ecol. Biogeogr.* **2004**, *13*, 345–358. [[CrossRef](#)]
45. Ge, Y.; Xu, F.; Zhuang, J. HiWATER: Dataset of investigation on channel flow and socio-economy in the middle reaches of the Heihe River Basin. *Heihe Plan Sci. Data Cent.* **2013**. [[CrossRef](#)]
46. Ge, Y.; Zhuang, J.; Ma, C.; Xu, F. HiWATER: Dataset of investigation on crop phenology and field management in the middle reaches of the Heihe River Basin. *Heihe Plan Sci. Data Cent.* **2013**. [[CrossRef](#)]
47. Xu, T.; Liu, S.; Xu, L.; Chen, Y.; Jia, Z.; Xu, Z.; Nielson, J. Temporal upscaling and reconstruction of thermal remotely sensed instantaneous evapotranspiration. *Remote. Sens.* **2015**, *7*, 3400–3425. [[CrossRef](#)]
48. Rosa, R.D.; Paredes, P.; Rodrigues, G.C.; Alves, I.; Rui, M.F.; Pereira, L.S.; Allen, R.G. Implementing the dual crop coefficient approach in interactive software. 1. Background and computational strategy. *Agric. Water Manag.* **2012**, *103*, 8–24. [[CrossRef](#)]
49. Allen, R.G.; Pereira, L.S.; Raes, D.; Smith, M. *Crop Evapotranspiration—Guidelines for Computing Crop Water Requirements—FAO Irrigation and Drainage Paper 56*; FAO—Food and Agriculture Organization of the United Nations: Rome, Italy, 1998; p. 6541.
50. Rosa, R.D.; Paredes, P.; Rodrigues, G.C.; Rui, M.F.; Alves, I.; Pereira, L.S.; Allen, R.G. Implementing the dual crop coefficient approach in interactive software: 2. Model testing. *Agric. Water Manag.* **2012**, *103*, 62–77. [[CrossRef](#)]
51. Arnold, J.G.; Srinivasan, R.; Muttiah, R.S.; Williams, J.R. Large area hydrologic modeling and assessment part I: Model development. *JAWRA J. Am. Water Resour. Assoc.* **1998**, *34*, 73–89. [[CrossRef](#)]
52. Williams, J. The erosion-productivity impact calculator (EPIC) model: A case history. *Philos. Trans. R. Soc. London. Ser. B Biol. Sci.* **1990**, *329*, 421–428. [[CrossRef](#)]
53. Abbaspour, K.C.; Vejdani, M.; Haghghat, S. SWAT-CUP calibration and uncertainty programs for SWAT. In *MODSIM 2007 International Congress on Modelling and Simulation*; Modelling and Simulation Society of Australia and New Zealand Inc.: Canberra, Australia, 2007; pp. 1603–1609.
54. Izady, A.; Davary, K.; Alizadeh, A.; Ziaei, A.; Akhavan, S.; Alipoor, A.; Joodavi, A.; Brusseau, M. Groundwater conceptualization and modeling using distributed SWAT-based recharge for the semi-arid agricultural Neishaboer plain, Iran. *Hydrogeol. J.* **2015**, *23*, 47–68. [[CrossRef](#)]
55. Neitsch, S.; Arnold, J.; Kiniry, J.; Williams, J.; King, K. *Soil and Water Assessment Tool: Theoretical Documentation Version 2005*; Texas Water Resources Institute: College Station, TX, USA, 2005.
56. Dechmi, F.; Burguete, J.; Skhiri, A. SWAT application in intensive irrigation systems: Model modification, calibration and validation. *J. Hydrol.* **2012**, *470*, 227–238. [[CrossRef](#)]
57. Liu, Y.; Pereira, L.; Fernando, R. Fluxes through the bottom boundary of the root zone in silty soils: Parametric approaches to estimate groundwater contribution and percolation. *Agric. Water Manag.* **2006**, *84*, 27–40. [[CrossRef](#)]
58. Duan, A.; Sun, J.; Liu, Y.; Xiao, J. *The Main Crop Irrigation Water Quota in Northern Area*; China Agricultural Science and Technology Press: Beijing, China, 2004. (In Chinese)
59. Zhang, B.; Xu, D.; Liu, Y.; Li, F.; Cai, J.; Du, L. Multi-scale evapotranspiration of summer maize and the controlling meteorological factors in north China. *Agric. For. Meteorol.* **2016**, *216*, 1–12. [[CrossRef](#)]
60. Zhang, Y.; Zhao, W.; He, J.; Zhang, K. Energy exchange and evapotranspiration over irrigated seed maize agroecosystems in a desert-oasis region, northwest China. *Agric. For. Meteorol.* **2016**, *223*, 48–59. [[CrossRef](#)]
61. Vazquez-Amabile, G.; Engel, B. Use of SWAT to compute groundwater table depth and streamflow in the Muscatatuck River watershed. *Trans. ASAE* **2005**, *48*, 991–1003. [[CrossRef](#)]

62. Kannan, N.; White, S.; Worrall, F.; Whelan, M. Sensitivity analysis and identification of the best evapotranspiration and runoff options for hydrological modelling in SWAT-2000. *J. Hydrol.* **2007**, *332*, 456–466. [[CrossRef](#)]
63. Neitsch, S.L.; Arnold, J.G.; Kiniry, J.R.; Williams, J.R. *Soil and Water Assessment Tool: Theoretical Documentation. Version 2009*; Texas Water Resources Institute: College Station, TX, USA, 2011.
64. Monsi, M.; Saeki, T. Uber den Lichtfaktor in den Pflanzengesellschaften und sein Bedeutung fur die Stoffproduktion. *Jpn. J. Bot.* **1953**, *14*, 22–52.
65. Simunek, J.; Saito, H.; Sakai, M. *The HYDRUS-1D Software Package for Simulating the One-Dimensional Movement of Water, Heat, and Multiple Solutes in Variably-Saturated Media*, version 3.0; Department of Environmental Sciences, University of California: Riverside, CA, USA, 1998.



© 2018 by the authors. Licensee MDPI, Basel, Switzerland. This article is an open access article distributed under the terms and conditions of the Creative Commons Attribution (CC BY) license (<http://creativecommons.org/licenses/by/4.0/>).